J. Univ. Kuwait (Sci.) **20**, 1993

The limit state analysis of containment vessel under accidental pressures

Y. F. AL-OBAID

Faculty of Technological Studies, PAAET, P.O. Box 42325, Shuwaikh 70654, Kuwait

ABSTRACT

The limit state analysis is proposed in this paper. The analysis takes into consideration two types of dome namely, spherical and elliptical, which are generally associated with the barrel wall. Constitutive equations are developed in which a provision is made for tendon geometry, loads and losses due to prestressing tendons. Stresses are computed for the domes and the barrel wall using a specially developed program (HAYA). A separate analysis is carried out for the discontinuity at the base of the barrel wall. Boundary conditions are adjusted so as to create flexibility for the dome and wall to interact. The analysis is applied to both Sizewell B and Bellefonte vessels. Only Bellefonte vessel results are reported.

INTRODUCTION

The state of the art review of containment vessels for pressurized water reactor (PWR) and boiling water reactor (BWR) is fully reported by various authors (Al-Obaid 1984, 1986, 1989; Brading & Hills 1969; Stevenson 1980a). Several methods of analysis and design are discussed by Al-Obaid (1984, 1989, 1992), Brading & Hills (1969) and Stevenson (1980a, 1980b). They are mutually compared as part of a unified integrity assessment. The cracking conditions of such vessels under the influence of external impact are given (Al-Obaid 1989, 1992). The analytical and design tools thus available have made it possible to investigate future generating of vessels for all kinds of extreme load.

The containment vessels are made of steel and concrete. Concrete vessels are divided into two classes, namely reinforced and pre-stressed vessels. The walls are of cylindrical shape with spherical, elliptical and topospherical domes. Fig. 1 shows a typical Bellefonte containment with spherical dome. For many cases a secondary dome is provided to protect the primary containment from external hazards and the public from the internal hazards. Loads and stress criteria and certain codes and standards are required to design such vessels and their components.

This paper proposes the limit state analysis which is given to design such containment vessels for any kind of load. The analysis is tested on two existing Sizewell B and Bellefonte vessels. Only Bellefonte vessel results are reported in this paper.

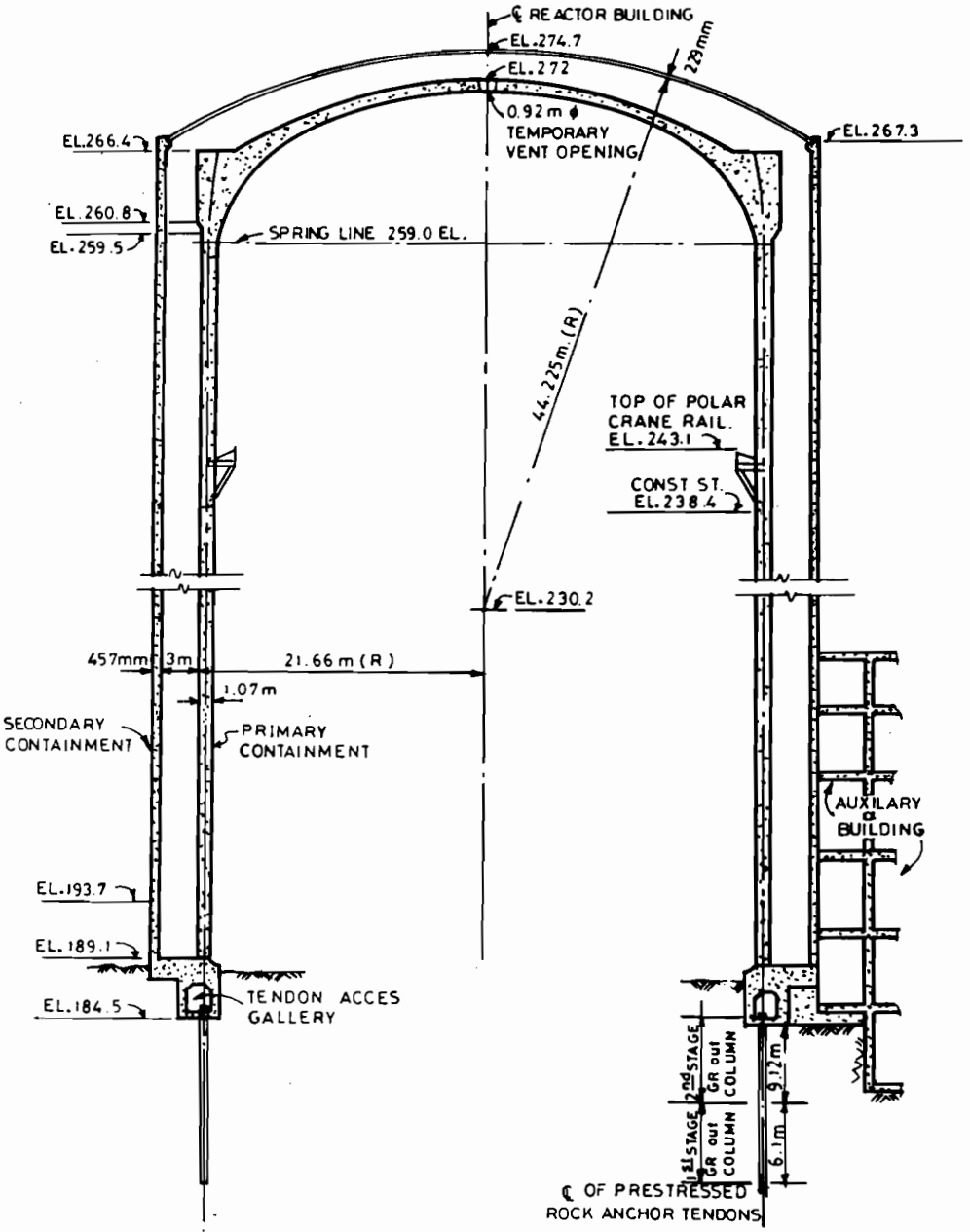

Fig. 1. Vertical presentation (Bellefonte vessel TVA).

LIMIT STATE ANALYSIS

The material from which the containment structure is constructed can be isotropic and non-isotropic. Also the structure of the containment vessel can be subjected to membrane actions and bending actions. In the membrane actions it is assumed that

the shell of the containment is incapable of withstanding any bending movements and the external loads are carried by internal forces induced in the surface of the containment shell only. On the other hand, the bending can only be resisted by the internal movements and forces induced in the containment shell.

The analysis given in this section can be applied both for static and dynamic conditions. These equations can easily be altered to suit the dynamic load effects. Both spherical cylinder and ellipsoidal cylinder analyses are included. The steps for limit state analysis are:

1. DOMES

The containment vessels carry two types of dome. The equations for meridional and hoop stresses for spherical and elliptical or topospherical domes can be derived as follows:

(A) Spherical dome

Take an element in the middle surface of the shell revolution where

r = radius of curvature of parallel circle
a = radius of curvature of meridian

Fig. 2 shows the membrane stress resultants and the load of components

$$P_X, P_Y, P_Z$$

The co-ordinate axes are:

X = along tangent to parallel circle
Y = along tangent to meridian

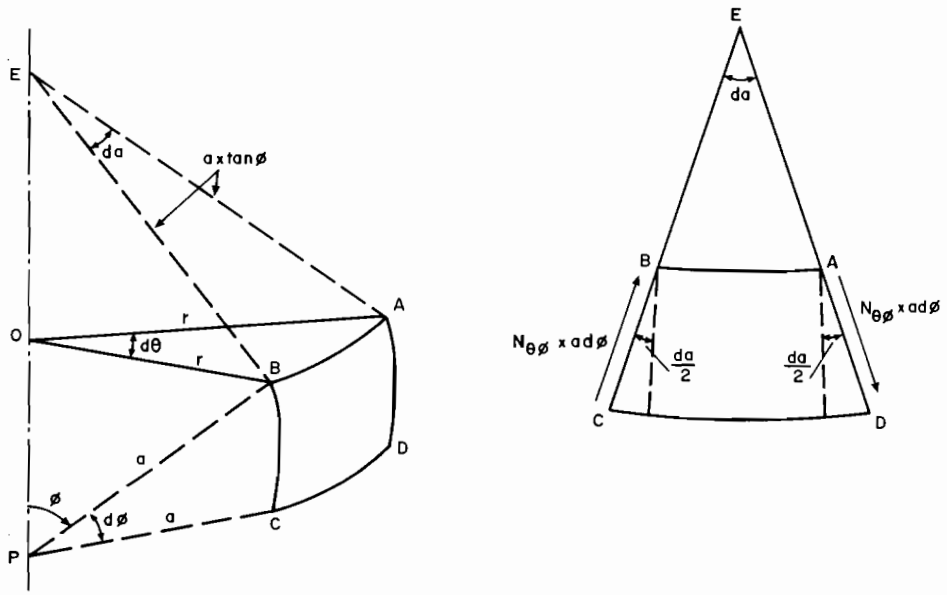

Fig. 2. Side element equilibrium.

Z = normal to shell surface

The complete derivation of the equations of meridional and hoop stress for spherical and ellipsoidal shell can be found in Pfluger (1961), Billington (1982), and Kelkar & Sewell (1987).

The equations of equilibrium of the element of a shell of revolution can be shown in Figs 2 to 5.

For forces in the direction of X, the equation of equilibrium is

$$\frac{\partial(N_{\phi\theta} r)}{\partial\phi} + \frac{\partial N_\theta}{\partial\theta} + aN_{\theta\phi} \cos\phi + P_x ra = 0. \tag{1}$$

The equation of forces in the direction of Y is

$$\frac{\partial(rN_\phi)}{\partial\phi} + \frac{a\,\partial N_{\theta\phi}}{\partial\theta} - N_\theta\, a \cos\phi + P_Y ra = 0. \tag{2}$$

For forces in the direction Z, the equation of equilibrium is

$$\frac{1}{a}(N_\theta + N_\phi) + P_Z = 0. \tag{3}$$

Assuming the stresses are uniformly distributed over the thickness of the shell

$$N_{\phi\theta} = N_{\theta\phi}. \tag{4}$$

Eqns (1), (2), (3) and (4) allow the calculation of the membrane forces of a shell of revolution. Hence, with loads symmetric about the vertical axis of rotation, the four equations simplify considerably:

(a) Stresses are independent of θ and all partial derivatives, with respect to θ, disappear.
(b) $N_{\phi\theta} = N_{\theta\phi} = 0$, because otherwise they would produce unsymmetrical deformation with respect to the vertical axis.
(c) There is no variation of other stress resultants with Q.
(d) The component P of the load must vanish; it would produce twist about the axis and shear deformation.

Therefore, Eqn (1) is identically satisfied and disappears. Hence Eqn (2) becomes

$$\frac{d}{d\phi}(rN_\phi) - aN_\theta \cos\phi + P_Y ra = 0. \tag{5}$$

Eqn (3) remains the same

$$\frac{1}{a}(N_\theta + N_\phi)P_Z = 0.$$

Therefore

$$N_\theta = -(P_Z a + N_\phi). \tag{6}$$

For a dome which is symmetrically loaded on the axis, the meridional force N_ϕ can be obtained much faster and directly by considering the equilibrium of the part of the dome above a certain parallel circle.

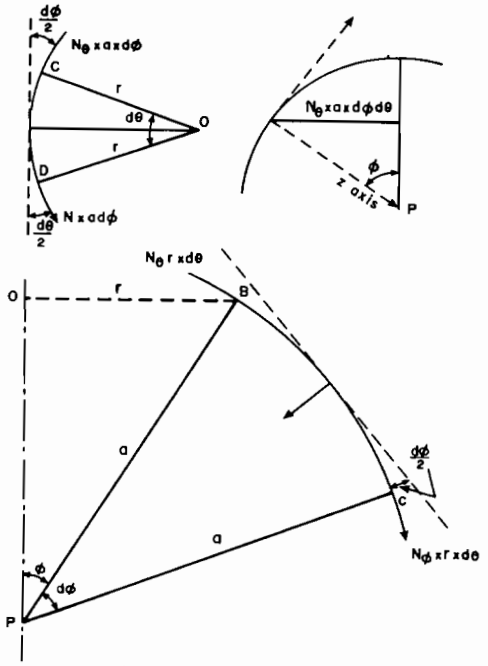

Fig. 3. Curve on longitude.

Then, if V is the vertical resultant of the applied load and $2\pi r N_\phi \sin\phi$ is the total vertical component around the parallel circle of the meridional force N_ϕ

$$N_\phi = -\frac{-V}{2\pi r \sin\phi}. \tag{7}$$

Let W = weight per unit area
$S_\phi = 2\pi aH$
$= 2\pi a^2(1 - \cos\phi)$ = surface area above parallel
$4\pi r^2$ = surface area of sphere
$\frac{4}{3}\pi r^3$ = volume of sphere.

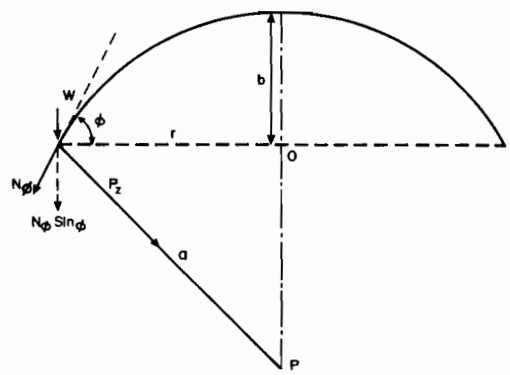

Fig. 4. Dome

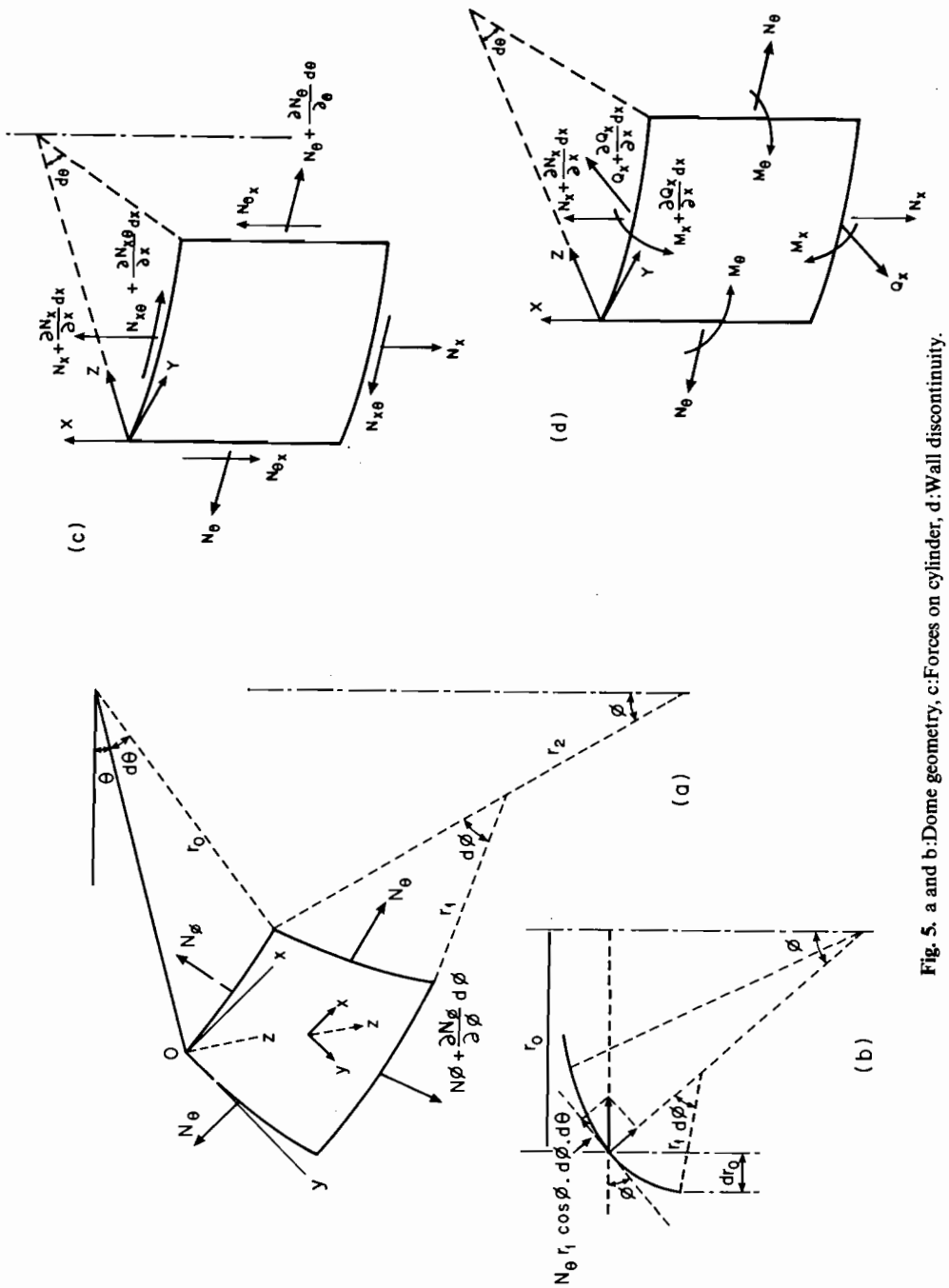

Fig. 5. a and b:Dome geometry, c:Forces on cylinder, d:Wall discontinuity.

Therefore, the load above parallel is

$$V = WS_\phi$$
$$= 2\pi Wa^2(1 - \cos\phi). \tag{8}$$

Therefore, the meridional force is

$$N_\phi = -\frac{Wa}{1 + \cos\phi}. \tag{9}$$

and the hoop force is

$$N_\theta = Wa\left(\frac{1 - \cos\phi - \cos^2\phi}{1 + \cos\phi}\right) \tag{10}$$

(*B*) *Ellipsoidal dome*

In order to differentiate from the spherical dome, some symbols for radii are changed and have been renamed for the ellipsoidal dome. Fig. 6 shows the element of such a dome. The position of a meridian is defined by meridional angle ϕ, as before. The meridional plane and the plane perpendicular to it are the planes of principal curvature. The corresponding radii of curvature are r_1 and r_2 respectively. The radius of a parallel circle is denoted by r_θ.

With symmetrical loading it can be concluded that there will be no shearing forces acting on the sides of the element. The external load in the meridian plane is resolved in Y and Z directions. The normal forces to the sides of the element are N_ϕ and N_θ.

The force in Y-direction (Fig. 5b) is

$$\left(\frac{d}{d\phi}\right)(N_\phi r_0) - N_\theta r_1 \cos\phi + Y r_1 r_0 = 0. \tag{11}$$

For forces in Z direction (Fig. 5b), the equation of equilibrium is

$$\frac{N_\phi}{r_1} + \frac{N_\theta}{r_2} = -Z. \tag{12}$$

This equation is identical to Eqn (3).

The above equations can be used to determine N_ϕ and N_θ. The radii of curvature $r_1 r_2$ can be calculated from (13) and (14) below

$$r_1 = \frac{a^2 b^2}{(a^2 \sin^2\phi + b^2 \cos^2\phi)^{1/2}} \tag{13}$$

$$r_2 = \frac{a^2}{(a^2 \sin^2\phi + b^2 \cos^2\phi)^{1/2}}. \tag{14}$$

Now, if P is the uniform internal pressure, then for any parallel circle of r_0 we have

$$R = -\pi P r_0^2$$

and (12) gives

$$N_\phi = \frac{Pr_0}{2\sin\phi} = \frac{Pr_2}{2}. \tag{14a}$$

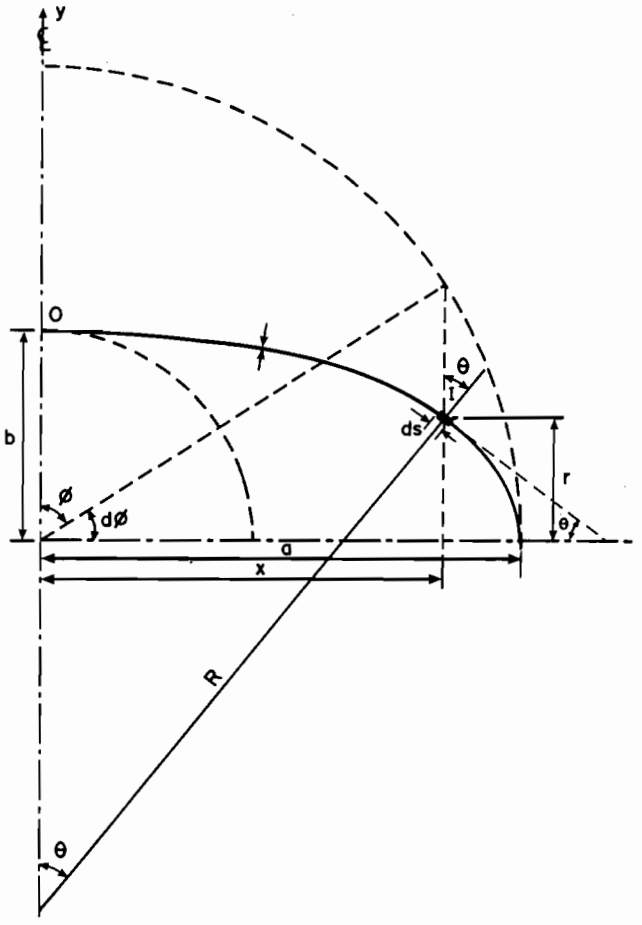

Fig. 6. Elliptical dome geometry.

And substituting into (12) we obtain

$$N_\theta = Pr_2 - \frac{r_2 N_\phi}{r_1}$$

$$N_\theta = P\left(r_2 - \frac{r_2^2}{2r_1}\right). \tag{14b}$$

Eqns (14a) and (14b) can be used to determine the meridional and hoop forces at any point along the dome provided the major and minor axes a, b are known and that the internal pressure P is given.

Now we determine the meridional and hoop forces (see Fig. 6).

Let w = weight of dome surface/unit area
MTD = meridional thrust due to dead load
HTD = hoop thrust drive to dead load.

Total dead load of dome = $WD = 2\pi a^2 wc$, where a = major axis, c = a constant (Fig. 6). $WD = \sum$ vertical components of MTD = MTD $\times 2\pi \sin\theta$.

$$\tan\theta = \frac{dy}{dx} = -\frac{b \sin\phi \, d\phi}{c \cos\phi \, d\phi} = -\frac{-b^2 x}{a^2 y}$$

where b = minor axis

$$\sin\theta = \frac{b[1-(y/b)^2]^{1/2}}{a\{1-(a^2-b^2)^2[1-(y/b)^2]\}^{1/2}}$$

$$\text{MTD} = \frac{WD}{\sin\theta 2\pi} = \frac{a^2 wc}{b[1-y/b)^2]} \times \frac{(1-(a^2-b^2)^2/a^2 1-(y/b)^2)^{1/2}}{Q_0} \tag{15}$$

$$\text{MTD} = \frac{a^2 WCQ_0}{b(1-[y/b]^2)}. \tag{16}$$

At point I (Fig. 7)

$$\frac{\text{MTD}}{R} + \frac{\text{HTD}}{X}\sin\theta - W\cos\theta = 0. \tag{17}$$

R = radius of curvature.
Substituting (16) into (17) we have

$$\text{HTD} = -\frac{-WD}{2\pi R \sin^2\theta} + wa^2 y\{(y/b)^2 + \frac{b^2}{a^2}[1-(y/b)^2]\}. \tag{18}$$

But R, radius of curvature

$$= \left\{1 + \frac{(dy)^2}{(dx)}\right\}^{1/2} \Big/ \frac{d^2 y}{dx^2}$$

$$\frac{dy}{dx} = \frac{b^2}{a^2}\frac{x}{y} \Rightarrow R = b\{1-(y/b)^2\} \times \left\{1 - \frac{(a^2-b^2)^2}{a^2}(1-(y/b)^2)\right\}^{1/2}. \tag{19}$$

Substituting (18) into (19)

$$\text{HTD} = \frac{wa^2}{b} \times \left[y/b - \frac{c}{\{1-(y/b)^2\}\{1-(a^2-b^2)^2/a^2\}\{1-(y/b)^2\}^{1/2}}\right] \tag{20}$$

$$\text{HTD} = \frac{Wa^2}{b}\left\{\frac{y}{b} - \frac{c}{\{1-(y/b)^2)}Q_0\right\}.$$

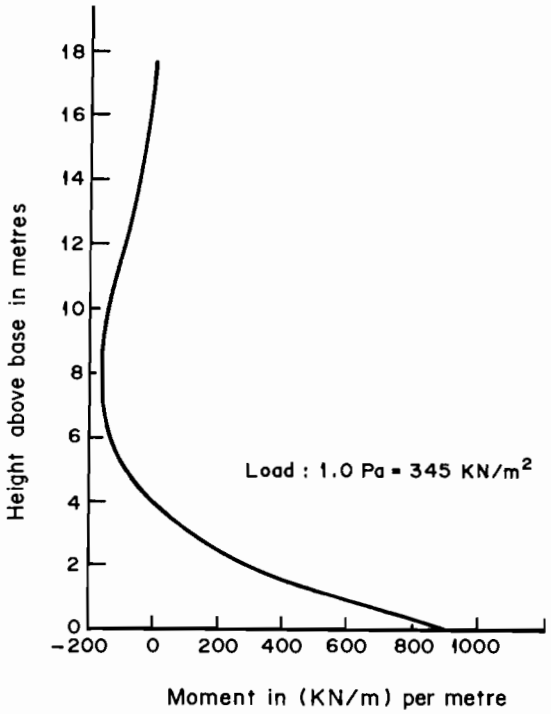

Fig. 7. Discontinuity moment at the bottom of cylinder.

Meridional thrust due to live load

$$MTL = \frac{W1a^2}{2b} Q_0. \tag{21}$$

Hoop thrust due to live load

$$HTL = \frac{W1a^2}{2b} \frac{\{2(y/b)^2 - 1)\}}{Q_0} \tag{22}$$

where $W1$ = live load on domed surface per unit area.

2. BARREL WALLS

Analysis of the barrel wall is based on the energy dissipation technique. Three possibilities are considered.

(a) Failure of the barrel wall while there is still a compressive axial load from the prestressing cables and dome reactions.
(b) Failure due to rupturing of the prestressing cables.
(c) Failure under concrete cracking.

The wall is located as an infinitely long cylinder; the general displacement equation is derived using the uniformly distributed load obtained from the hoop tendons as shown in Fig. 8.

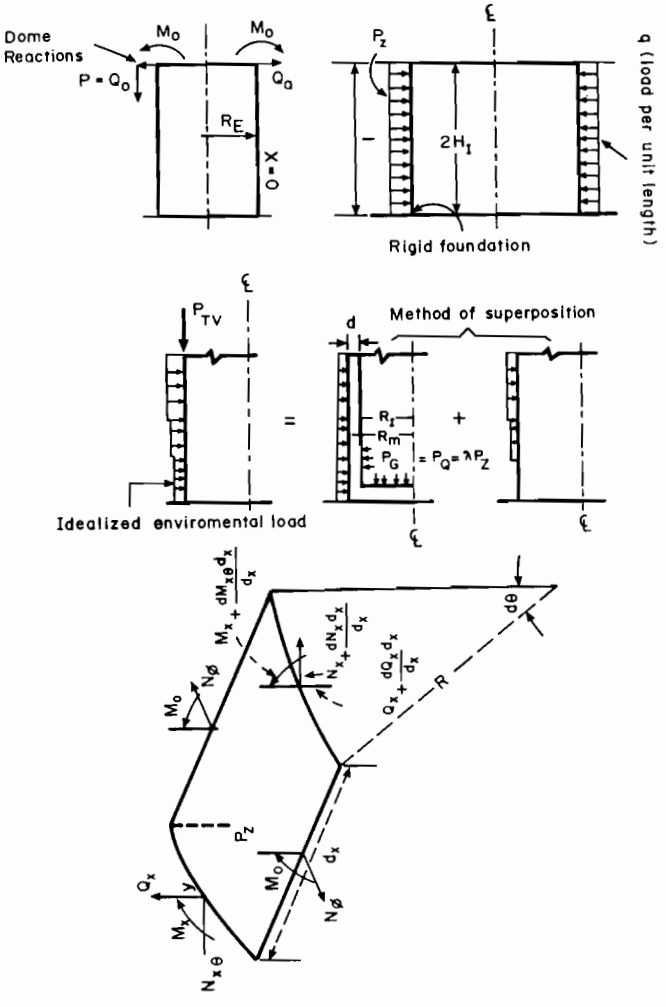

Fig. 8. Forces on barrel wall.

$$W = \frac{P_x R^2}{Et}\left(-\theta(\beta x) - \xi(3X) + 1\right) \tag{23}$$

The force $N_{\theta 1}$ in the circumferential direction is given as

$$\begin{aligned} N_{\theta 1} &= \frac{Etw}{R} \\ &= -P_x R(1 - \xi(\beta X) - \theta(\beta X)) \\ &= -P_x R(1 - e^{-\beta x} \sin \beta X - e^{-\beta x} \cos \beta X) \end{aligned} \tag{24}$$

where P_x is a load system.

From the second and third derivatives of Eqn (23), the following bending moment and shearing force can be obtained:

$$M_{x1} = -D\frac{d^2w}{dx^2}$$

$$\frac{dw}{dx} = (2\beta e^{-\beta x} - \sin\beta x)\frac{P_x R^2}{Et}$$

$$-D\frac{d^2w}{dx^2} = -D(+2\beta^2 e^{-\beta n}\cos\beta n - 2\beta^2 \sin\beta x e^{-\beta n})\frac{P_x R^2}{Et} \tag{26}$$

$$= 2\beta^2 D(\xi(\beta x) - \theta(\beta x) \times \frac{P_x R^2}{Et}$$

$$Q_{x1} = \frac{dMx}{dx} = -D\frac{d^3w}{dx^3} = 4\beta^3 D\frac{P_x R^2}{Et}\theta(\beta x). \tag{27}$$

Due to the dome the outward forces P can be developed. This will have an effect on the loaded state of the cylinder where the bending (M_0) and shearing (Q_0) forces involved in the final expression for w are

$$w = \frac{1}{2\beta^3 D}(M_0\{\xi(\beta x') - \theta(\beta x')\} - Q_0\,\theta(\beta x')) \tag{28}$$

where Q_0 = discontinuity shear.

The slope at the loaded end is obtained by differentiating Eqn (28) which gives

$$\frac{(dw)}{dx}x' = 0 = \frac{1}{2\beta^2 D}(2\beta\theta(\beta x') + Q_0\,\theta(\beta x') + \xi(\beta x'))x' = 0$$

$$= \frac{1}{2\beta^2 D}(2\beta M + Q_0);\ D = \text{stiffness}. \tag{29}$$

From considerations of symmetry and loads, the value of Q_0 in this case is

$$Q_0 = P/2(-P_Q). \tag{29a}$$

The right hand side of Eqn (28) is thus obtained

$$w = \frac{1}{2\beta^3 D}(\beta M_0(\xi(\beta x') - \theta(\beta x')) - P_Q\,\theta(\beta x')) \tag{30}$$

To calculate the moment M_0 which appears in Eqn (30), use Eqn (29).

In this case, the slope vanishes because of symmetry. Hence

$$2\beta M_0 + P_Q = 0.$$

Hence

$$M_0 = -\frac{P_Q}{2\beta};\qquad P_Q = \text{accidental pressure} = \lambda P_Z. \tag{31}$$

Substituting Eqn (31) into Eqn (30), the displacement is

$$w = \frac{-P_Q}{4\beta^3 D}(\xi(\beta x') + \theta(\beta x')). \tag{32}$$

Therefore

$$N_{\theta 2} = -\frac{Etw}{R} = \beta R P_Q \times (\xi(\beta x') + \theta(\beta x') \tag{33}$$

$$M_{X2} = -D\frac{d^2w}{dx^2} = \frac{P_Q}{2\beta}(\xi(\beta x') - \theta(\beta x') \tag{34}$$

$$Q_{X2} = -D\frac{d^3w}{dx^3} = P_Q\theta(\beta x') \tag{35}$$

The direct load P_T (Fig. 8) is a reaction from the dome. They are the additional forces which must be included in the above formulation. In brief they are given below.

The load due to vertical prestressing does have an influence on the flexural and shear behavior of the wall. Based on energy dissipation, the following interaction equation has been obtained:

$$K_w = 942 \times 10^{-6}\frac{P_{TV}}{R_E^a}[n' + n'_1\cos\theta_1 + n'_2\cos\theta_2] \tag{36}$$

$$\bar{K}_w = 4{\cdot}7 \times 10^3\left[\frac{R_m}{R_1}\left(\frac{(H^21)}{R_m R_1\, d^2} - 2K_w + 1\right)^2\right. \tag{37}$$

$$+ 4(32P_s + \bar{K}_w - K_w^2) + \frac{2H_1^2}{R_m^2 d^2}(34P_s + H_p)^{1/2})$$

$$\left. + \frac{R_m}{R_1}(2K_w - 1)\right] - \frac{H_1^2}{R_1\, d^2}\Bigg] \tag{38}$$

where $H_p = \bar{P}_H\left(\dfrac{R + 1250}{4700d}\right)$

$\bar{P}_H = 0{\cdot}9P''_H f, H$

$P''_H =$ (average pressure)

$= \dfrac{S_n T(\text{or } P_{TV})}{12R'_E B}$

$P_w(\text{ult})/P_Q =$ load factor

$B =$ band width or hoop tendons spacing

$d =$ wall thickness (m)

$f =$ incremental factor up to ultimate level for vertical prestressing

$f_1 =$ incremental factor up to ultimate level for circumferential prestressing

$fcu =$ average compressive stress at hinge at the junction of wall and cap

$H_1 =$ half of internal height (m)

$K_w, \bar{K}_w =$ parameters

$n'_1, n'_2 =$ number of curved vertical tendons in rows

$n =$ number of vertical tendons

$\theta_1\theta_2 =$ inclination to vertical of tendons in rows

$P_{TV} =$ ultimate load of a vertical tendon

$P'_H =$ ultimate load of circumferential prestressing

$P_s =$ % of high tensile bonded reinforcement

P_H, P''_H = average pressure in a circumferential direction on the external faces of wall and cap respectively.
P_w (*ult*) = minimum ultimate pressure which the wall would take
η = factor defining the relationship during deformation of the vessel between ultimate load of prestressing system, effective radius or radii and average pressure on the external face of the vessel
R_1, R_E = effective internal and external radii respectively
R_m = radius to the centroid of vertical tendons
S_n = number of strands or wires or tendons in the hoop direction
T = ultimate load in strands or wires

DESIGN LOAD CRITERIA AND VESSELS DATA

(1) Design loads and stresses
$D + F + 1{\cdot}5P_a + T_a$
$D + F + 1{\cdot}25P_a + T_a + 1{\cdot}25E$
$D + F + P_a + T_a + E$
D + dead load; F − prestressing loads;
P_a − local pressure; T_a − local temperature load;
E − seismic (OBE) load; E' seismic (SSE)
P_a = 50 psig; design accident temperature 271°F
E − 0·05g; $E = 0{\cdot}11g \uparrow$ and $0{\cdot}17 \rightarrow$; time 100 seconds
E^* (SSE) uplift 6.9 MN/m; f_{cu} = 41·3 MN/m^2
E_c = 28 MN/m^2; E_s = 200 GN/M^2
E (OBE) = uplift 4·7 MN/m
$\mu = 0{\cdot}14$, $K = 0{\cdot}0003$ for friction; tendon losses 21%
Bellefonte a = 69·125 ft (21·07 m), b = 41·375 ft (12·6 m)
Containment wall hoop prestressing (initial) 9900 kN/m^2
Dome prestressing (meridional) 5000 kN/m
75% lock off.

Parameter	*Bellefonte vessel* (topospherical)	*Sizewell B* (spherical)
R_1	21·66 m	22·50 m
d (wall)	1·07 m	2·50 m
R (outer dome)	44·225 m	22·860 m
d (dome)	229 m	1500 mm

RESULTS

The results obtained from Program HAYA for the dome and the wall are given in Figs 9 and 10. Sixteen increments for the values of f and f_1 are considered in order to obtain the results. The following load factors are reported:

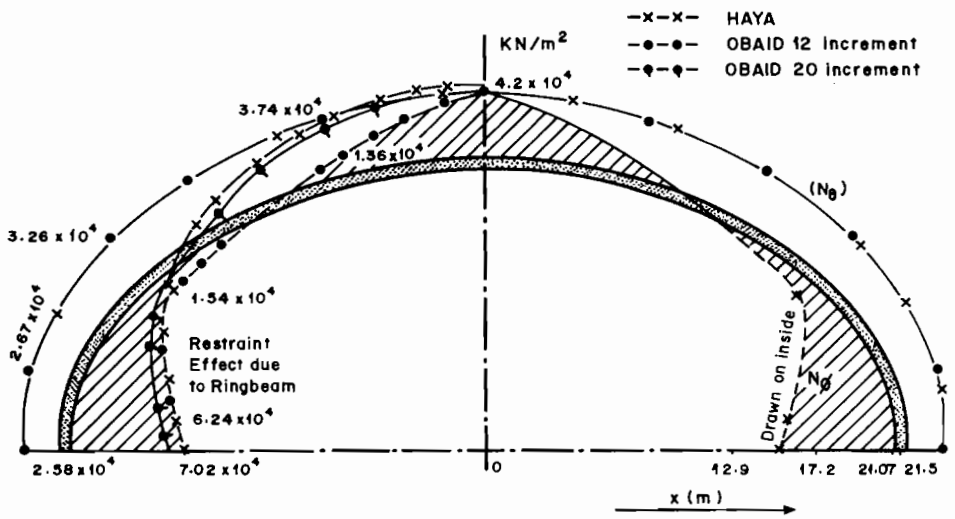

Fig. 9. Stress distribution on dome.

Basement shear	1·57
Wall	1·85
Concrete cracking wall	3·90
Dome compression	5·80
Prestressing tendon load	2·50

These results are compared with the three-dimensional finite element analysis in Fig. 9 from Program OBAID.

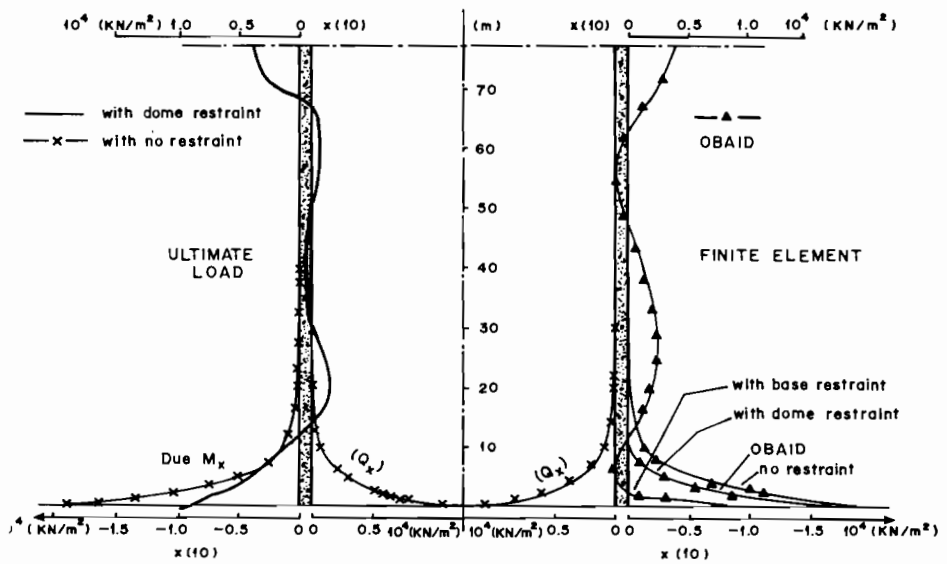

Fig. 10. Stress on barrel wall.

SUMMARY AND CONCLUSIONS

Due to the limitation of space, it was not possible to give detailed information on the vessels layout and design calculations, particularly for the Sizewell B. However, the subject of the ultimate load analysis based on limit state is introduced. More research is needed to evaluate additional design areas. The load factors or safety margins obtained are in good agreement with those from the finite element analysis (Al-Obaid 1989).

REFERENCES

Al-Obaid, Y.F. 1984. Dynamic crack propagation in PWR tube. Pressure Vessel and Piping Conference (ASME), June 17–21, Houston, Texas, U.S.A.

Al-Obaid, Y.F. 1986. The finite element analysis of crack growth in zircaloy tubing under extreme temperature. International Journal of Engineering Fracture Mechanics **23(5)**: 875–82.

Al-Obaid, Y.F. 1989. Aircraft impact analysis of the proposed Sizewell B containment vessel. Third Conference on Aeronautical Sciences and Aviation Technology, April 4–6, Cairo, Egypt.

Al-Obaid, Y.F. 1992. Three-dimensional cracking analysis of concrete containment vessels under external impacts. The Journal of the University of Kuwait (Science) **19(1)**: 17–34.

Billington, D.P. 1982. Thin shell concrete structures. McGraw-Hill, New York.

Brading, K.F. & Hills, G. 1969. Elastic and ultimate pressure tests on the tenth scale model of the Dungeness B concrete pressure vessel. Model Techniques for Prestressed Concrete Pressure Vessel Conference Proceedings BNES, London, UK.

Kelkar, V.S. & Sewell, R. 1987. Fundamentals of the analysis and design of shell structures. Prentice-Hall, New York.

Pfluger, V.S. 1961. Elementary statics of shells. F.D. Dodge Corporation, New York.

Stevenson, J.D. 1980a. Current summary of international extreme load design requirements for nuclear power plant facilities. International Journal of Nuclear Engineering and Design **60(1)**: 167–209.

Stevenson, J.D. 1980b. Structural damping values as a function of dynamic response stress and deformation values. International Journal of Nuclear Engineering and Design **60(2)**: 211–37.

(Received 4 March 1990, revised 24 June 1992)

تحليل الحد الأقصى
لقدرة تحمل الأوعية الاحتوائية الخرسانية
تحت تأثير الضغوط العرضية

يعقوب فهد العبيد
كلية الدراسات التكنولوجية
الهيئة العامة للتعليم التطبيقي والتدريب
ص. ب. 42325، الشويخ 70654، الكويت

خلاصة

يتناول هذا البحث بالتحليل مدى قدرة تحمل الأوعية الاحتوائية الخرسانية، كما يوضح ـ أيضا ـ نوعين من القباب: الكروية والبيضاوية، المرتبطة بالحوائط الأسطوانية.

ويتطرق البحث إلى الدراسة المستمرة لتطوير معادلات الأوتار الهندسية وقدرة التحمل والفاقد بسبب الأوتار سابقة الأجهاد. كما تم حساب إجهادات الشد للقباب والحوائط الأسطوانية من خلال البرنامج المتطور (هيا) HAYA.

وتم اجراء تحليل منفصل للتوقف واللاستمرارية على أساس الحوائط الأسطوانية. ولقد تم تعديل الظروف المحيطة لإتاحة الفرصة لمرونة التفاعل بين القبة والحائط، ومدى إمكانية تأثير كل منها على الآخر. كما تم تطبيق هذا التحليل على كل من وعائي سايزويل Sizewell B وبيل فونت Bellefonte. ويقدم البحث تقريرا عن نتائج أوعية بيل فونت.